Research Article

Ze Zhang, Zilong Wang, Juntao Yu, Yang Luo*, Wenlong Yan, Yuanfei Yang, Tengfei Hu, Dunbo Yu*, and Li Wang

Research on the influence of trapezoidal magnetization of bonded magnetic ring on cogging torque

https://doi.org/10.1515/phys-2022-0223
received October 11, 2022; accepted December 25, 2022

Abstract: In this article, the influence of trapezoidal magnetization method on cogging torque of permanent magnet motor is studied. First, the structure is analyzed by analytical method to explain its mechanism of reducing cogging torque. Then, in order to verify the effectiveness of the formula, a six-slot four-pole motor is introduced for finite element analysis. Through comparison of the original structure motor, the magnet skew structure motor, and the trapezoidal magnetic pole structure motor, it demonstrates that the trapezoidal magnetic pole structure motor can effectively reduce the Cogging torque and does not produce additional axial electromagnetic force. Finally, a magnetizing fixture with a trapezoidal magnetic pole structure is made to magnetize the magnetic ring. The magnetized magnetic ring is installed on the motor, and the Cogging torque, Back EMF, *etc*., are tested. The test results are in good agreement with the simulation results. This method can be used to optimize the cogging torque of the permanent magnet motor.

Keywords: axial electromagnetic force, back EMF, cogging torque, finite element analysis, trapezoidal magnetic pole

*** Corresponding author: Yang Luo,** General Research Institute for Nonferrous Metals, Beijing, China, e-mail: yudunbo@griam.cn
*** Corresponding author: Dunbo Yu,** General Research Institute for Nonferrous Metals, Beijing, China, e-mail: eluoyang@foxmail.com
Ze Zhang, Zilong Wang, Wenlong Yan, Yuanfei Yang, Tengfei Hu: National Engineering Research Center for Rare Earth, General Research Institute for Nonferrous Metals, Beijing, China
Juntao Yu, Li Wang: School of Mechanical, Electrical & Information Engineering, Shandong University (Weihai), Weihai, China

1 Introduction

compared with traditional motors, permanent magnet synchronous motors have the characteristics of high torque density, high efficiency, and fast dynamic response, and are widely used in servo drives such as automobiles. At the same time, the permanent magnet motor will generate cogging torque due to the interaction between the permanent magnet and the stator slot. The cogging torque always exists during the operation of the motor, which can cause problems such as vibration and noise [1,2].

At present, many scholars have proposed many methods to reduce the cogging torque. Such as slot skewing [3,4]: this method will increase the difficulty of stator processing and increase the amount of copper. Magnet skewing [5–9]: this method will increase the difficulty of processing and assembly for the magnetic tile, increase the cost, and will increase the extra-axial force of the motor. Magnetic pole shifting [10–13]: the rotor dynamic balance is affected and new harmonics are generated. Shifting the slot-openings [14]: manufacturing costs increase. As well as adjusting the shape of the slots or the tooth width [15,16], adding auxiliary slots or teeth [17], new modular stator fractional pole structure [18], axially tapered stator tooth tip [19], using unequal width magnetic poles [20], the slot and pole number combination [21], magnet pole clipping or sinusoidal magnetization [22], and optimizing cogging torque from a control perspective [23]. Regarding the analysis methods of cogging torque, there are currently energy methods [6], [24] and calculation methods of cogging torque based on Maxwell stress theory [25–27].

In sintered magnets, researchers have proposed trapezoidal pole distribution [28,29]. They all analyzed the structure from the angle that the trapezoidal magnetic pole provides sinusoidal flux linkage and sinusoidal back EMF, and did not give a specific angle calculation method. The larger the angle is, the better it is. The selection of trapezoidal pole distribution angle is related to the motor parameters.

Magnetic rings are widely used in micro-motors because of their high precision, low cost, and easy assembly [30,31]. Cogging torque also exists in motors using magnetic rings. Among the above-mentioned methods for reducing the cogging torque by optimizing the permanent magnet, the magnet skew is commonly used at present. The magnetic ring can realize the inclined pole magnetization of the magnetic ring by designing a magnetizing fixture. But the magnet skewing method will reduce the output torque of the motor and bring additional axial force. Because the bonded magnetic ring is very flexible, it can easily realize the trapezoidal magnetic pole distribution magnetization. Compared with traditional magnetization or magnet skew magnetization, the cost will not change.

In this article, by virtue of the flexible magnetizing characteristics of the bonded magnetic ring, the trapezoidal magnetic pole distribution of the bonded magnetic ring is directly realized through magnetization. The trapezoidal magnetic pole distribution magnetic ring is shown in Figure 1.

First, the structure is analyzed by analytical method to explain its mechanism of reducing cogging torque. Then, in order to verify the validity of the formula, a six-slot four-pole permanent magnet motor is introduced for finite element simulation analysis. The original structure motor, the magnet skew structure motor, and the trapezoidal magnetic pole structure motor are compared. The finite element calculation results show that the trapezoidal magnetic pole structure motor can effectively reduce the cogging torque without generating axial electromagnetic force. Finally, a magnetizing fixture with trapezoidal magnetic pole structure is made to magnetize the magnetic ring. The magnetized magnetic ring is installed in the motor and tested, and the test results are consistent with the simulation results.

2 Cogging torque minimization

2.1 Analytical method

Cogging torque is the torque produced by the interaction of the rotor permanent magnets with the stator cogging.

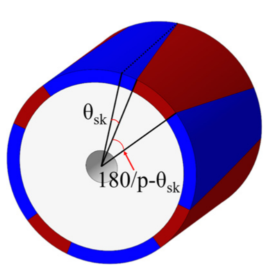

Figure 1: Trapezoidal magnetic pole structure.

The cogging torque is related to the rotor position and changes periodically with the rotor position.

In a surface mount permanent magnet brushless motor, it is assumed that 1) the magnetic permeability of the armature core is infinite, and 2) when not energized, the magnetic energy stored in the motor can be approximated as the sum of the magnetic energy in the permanent magnet (W_{pm}) and the air gap (W_{gap}):

$$W \approx W_{\mathrm{pm}} + W_{\mathrm{gap}} = \frac{1}{2\mu_0}\int_V B^2 \mathrm{d}V, \tag{1}$$

where μ_0 is the vacuum permeability. The distribution of the air gap flux density along the armature surface can be expressed as follows:

$$B(\theta, \alpha) = B_r(\theta)G(\theta, \alpha), \tag{2}$$

where $B_r(\theta)$ is the permanent magnetic remanence flux density distribution, α is the angle between the centerline of a specified armature tooth and the centerline of a specified permanent magnet, $G(\theta,\alpha)$ is the included angle between the magnetic pole centerline and the tooth centerline is α The distribution of the effective air gap length is reversed along the circumference of the circle. The cogging torque can be expressed as follows:

$$T_{\mathrm{cog}} = -\frac{\partial}{\partial\alpha}\left[\frac{1}{2\mu_0}\int_V B_r^2(\theta)G^2(\theta, \alpha)\mathrm{d}V\right], \tag{3}$$

where θ is the position angle. Expanding $B_r(\theta)$ and $G(\theta, \alpha)$ with Fourier series, respectively, the analytical expression of cogging torque can be obtained:

$$T_{\mathrm{cog}}(\alpha) = \frac{\pi z L_a}{4\mu_0}(R_2^2 - R_1^2)\sum_{n=1}^{\infty} nG_n B_{r(nz/2p)}\sin(nz\alpha), \tag{4}$$

where z is the number of slots, $2p$ is the number of poles, and L_a is the length of the core. In the inner rotor structure, R_1 and R_2 are the outer radius of the rotor yoke and the inner radius of the stator, and n is an integer that makes $nz/2p$ an integer.

The analysis shows that the number of fundamental cogging torque cycles γ in each revolution of the permanent magnet brushless motor rotor has the following relationship with the greatest common divisor (HCF) N_m of the number of stator slots z and the number of rotor poles $2p$:

$$\gamma = \frac{2pz}{N_m}. \tag{5}$$

Since the greatest common divisor N_m and the least common multiple (LCM) N_c have the following relationship:

$$2pz = N_c N_m. \tag{6}$$

Therefore, $\gamma = N_c$ that is, the number of fundamental wave cycles of the cogging torque when the rotor rotates one circle is equal to the least common multiple N_c of the number of stator slots z and the number of poles $2p$. The mechanical angle corresponding to the fundamental wave period of the cogging torque is $\theta_1 = 360°/N_c$ [32].

The cogging torque of the motor can be regarded as the sum of the interaction between each edge of the permanent magnet and the slot opening. It is well known that the magnet skew is an effective method to reduce the cogging torque. In order to completely eliminate the cogging torque, the skew angle of the magnet must be equal to the cycle of the cogging torque. In this way, when the magnetic pole conversion area of the permanent magnet passes through the stator slot, the magnetic pole conversion area is evenly distributed along the entire slot [33].

However, the skewing of the magnet will lead to the generation of axial electromagnetic force. If one of the magnetic pole conversion areas is tilted in the opposite direction, a magnetic ring with trapezoidal magnetic pole distribution can be obtained. When the two pole conversion areas of each pole of the magnetic ring with trapezoidal magnetic pole distribution pass through the notch, they are also evenly distributed. Therefore, the calculation formula of the skew pole angle of the trapezoidal magnetic pole structure should be the same as that of the traditional skew pole angle. As shown in Figure 1, the magnet skew angle of the trapezoidal magnetic pole structure is θ_{sk}. When the magnetic pole oblique angle θ_{sk} is equal to θ_1, the fundamental wave of cogging torque can be eliminated:

$$\theta_{sk} = \theta_1 = 360°/N_c. \tag{7}$$

2.2 Design of the Prototype

A six-slot four-pole permanent magnet motor is used for verification. This motor uses a bonded magnetic ring as a permanent magnet rotor. Bonded magnets can be classified into isotropic bonded magnets and anisotropic bonded magnets. Anisotropic bonded magnets are gradually being used in various micro-motors due to their high magnetic properties [30]. The magnetic rings used in this article are radially oriented anisotropic bonded magnetic rings.

The two-dimensional topology and three-dimensional cross-section of the motor used in this article are shown in Figure 2. The specifications for the motor are listed in Table 1.

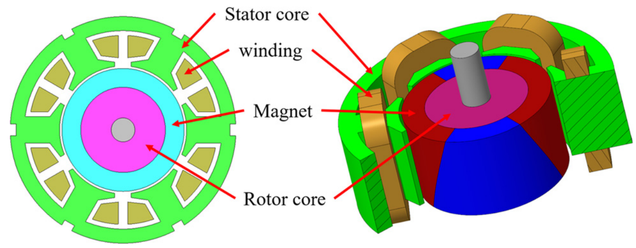

Figure 2: Two-dimensional topology map and three-dimensional cross-sectional view of the motor.

Table 1: Specifications of the motor

Item	Unit	Value
Stator slots	–	6
Magnet poles	–	4
Rated speed	rpm	18,000
Stator outer diameter	mm	48
Stator inner diameter	mm	27
Rotor diameter	mm	26
Inside diameter of magnet	mm	18
shaft diameter	mm	5
Motor axial length	mm	15

3 Finite element analysis

3.1 Verify the validity of the formula

The motor is modeled in finite element simulation software, and the 3D model specifications used in the simulation are consistent with the actual motor specifications. As shown in Figure 3, (a) is the 3D simulation model, (b) is the disassembled diagram of the model motor. In the simulation, the inclination angle range θ_{sk} of the trapezoidal magnetic pole structure is 0–50°, with a step size of 10°.

When θ_{sk} varies from 0–50°, the cogging torque changes as shown in Figure 4 below. It can be seen

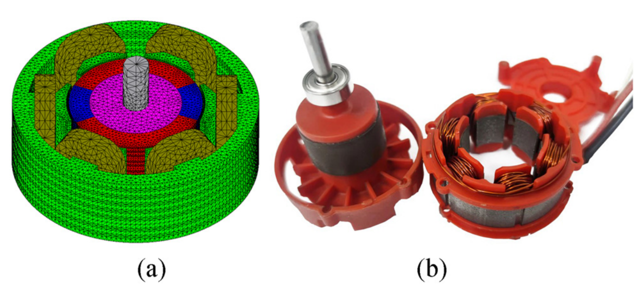

Figure 3: (a) 3D simulation model. (b) Disassembled prototype motor.

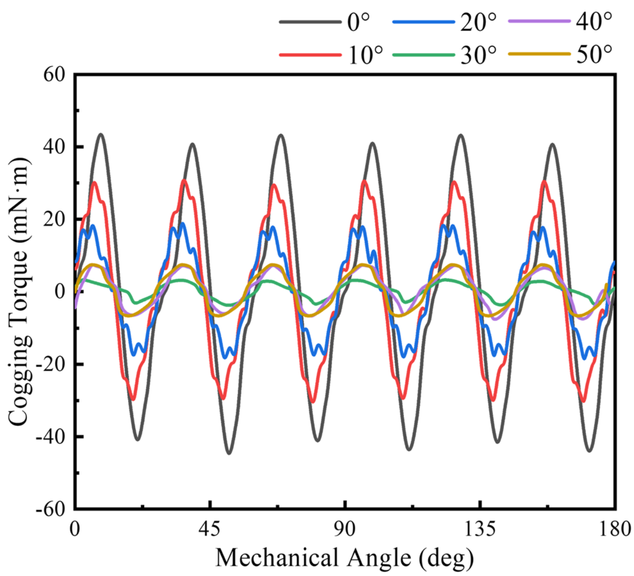

Figure 4: Relationship between cogging torque and magnet skew angle.

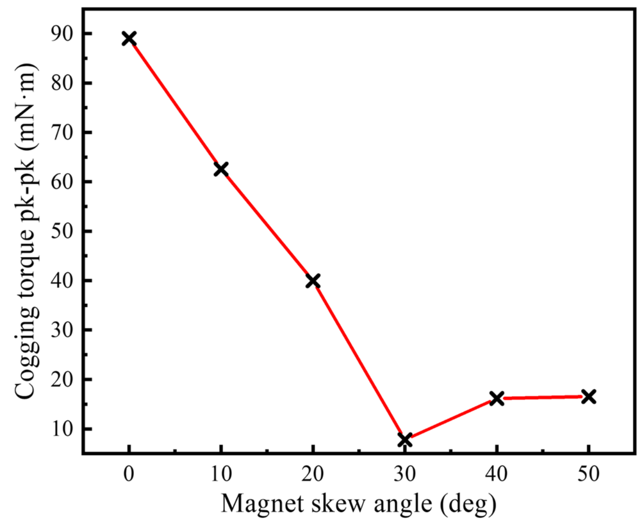

Figure 5: Curve of peak-to-peak value of cogging torque and magnet skew angle.

from Figure 4 that as the skew angle of the magnet increases, the amplitude of the cogging torque gradually decreases, and the period of the cogging torque does not change significantly.

The relationship between the peak-to-peak value of cogging torque and the skew angle of the magnet is shown in Figure 5.

It can be seen from Figures 4 and 5 that the cogging torque of the motor decreases with the increase of the skew angle of the magnet. When the skew angle θ_{sk} of the magnet is 30°, the peak-to-peak value of the cogging torque is the smallest. Subsequently, as the skew angle of the magnet increases, the peak-to-peak value of the cogging torque increases gradually. This result shows that formula (7) is suitable for the calculation of the magnet skew angle in the trapezoidal magnetic pole structure. This magnetic pole structure can be used to optimize the cogging torque of permanent magnet motors.

3.2 Comparison of cogging torque and rated output torque

Contrast trapezoidal magnetic pole structure with magnet skew structure and original structure (traditional four-pole structure) motors. As shown in Figure 6, (a) is the schematic diagram of the magnet skew structure motor when the magnet skew angle is 30°. (b) is the original structure motor.

The comparison between the cogging torque and the output torque of the three types of magnetic pole structure motors is shown in Figure 7 below.

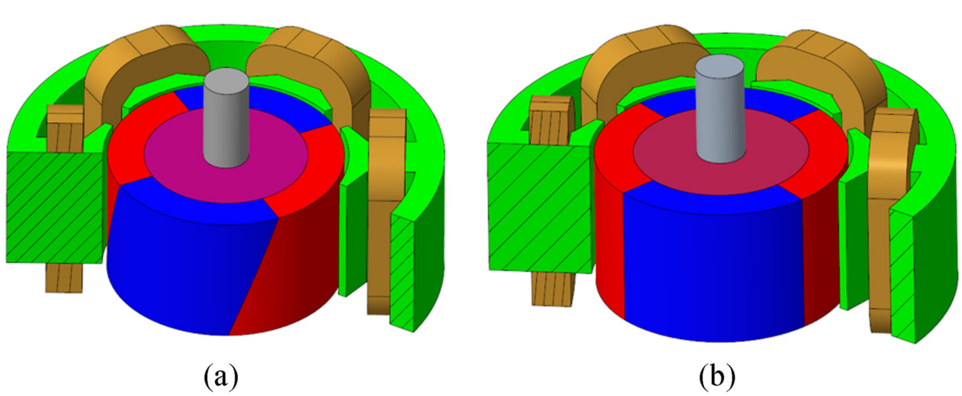

Figure 6: (a) Magnet skew structure motor. (b) Original structure motor.

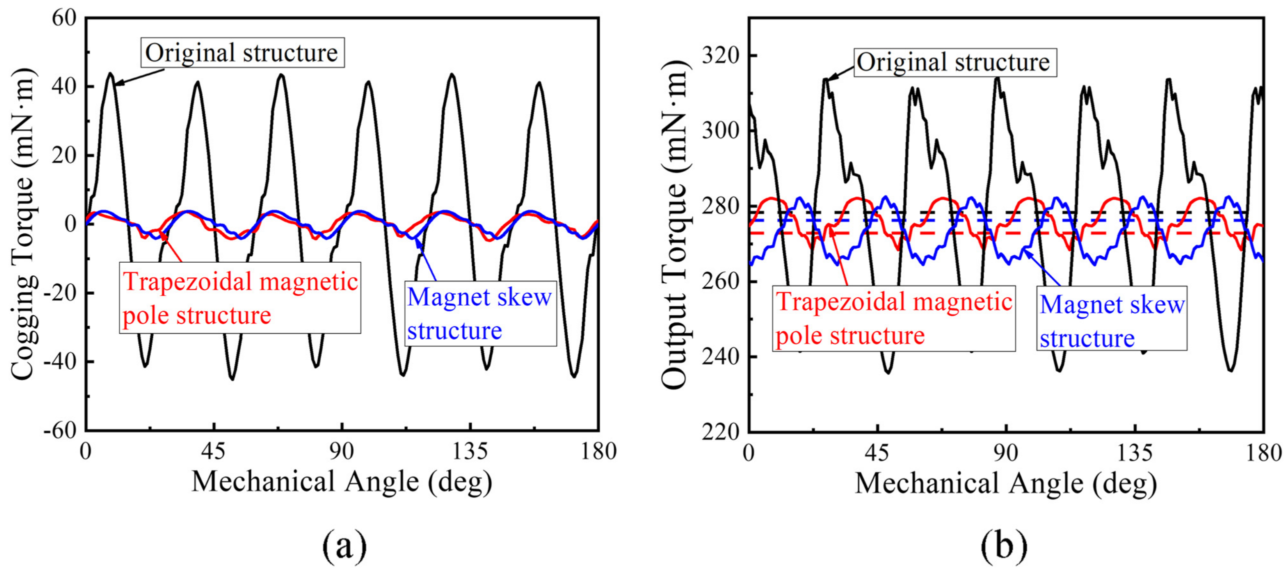

Figure 7: (a) Comparison of Cogging Torque; (b) comparison of Output Torque.

It can be seen from Figure 7(a) that the motor with trapezoidal magnetic pole structure can effectively reduce the cogging torque. It can be seen from Figure 7(b) that the torque ripple is significantly reduced, and the output torque is slightly decreased. Compared to the original structure, using the trapezoidal magnetic pole structure reduces cogging torque by 91.3%, while output torque decreases by 0.7%, magnet skew structure reduces cogging torque by 91.1% and output torque by 1.9%. It can be seen that the use of the trapezoidal magnetic pole structure can effectively reduce the cogging torque and at the same time reduce the drop of the output torque as much as possible.

3.3 Back EMF

The comparison of the Back EMF of the trapezoidal magnetic pole structure, the magnet skew structure, and the original structure motor is shown in Figure 8.

It can be seen from Figure 8 that the Back EMF waveform of the trapezoidal magnetic pole structure and the magnet skew structure is obviously more sinusoidal than the original structure motor. Fourier transform (FFT) analysis was performed on the Back EMF curve, and the result is shown in Figure 9.

It can be seen from Figure 9 that the fifth harmonic is the main harmonic, the amplitude of the 5th harmonic of

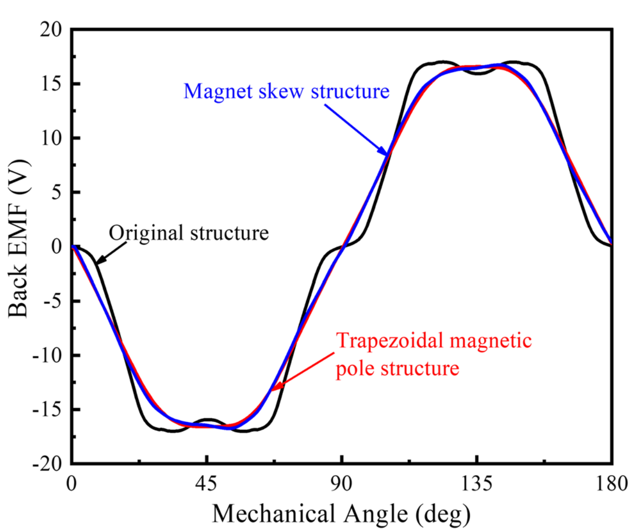

Figure 8: Back EMF simulation results.

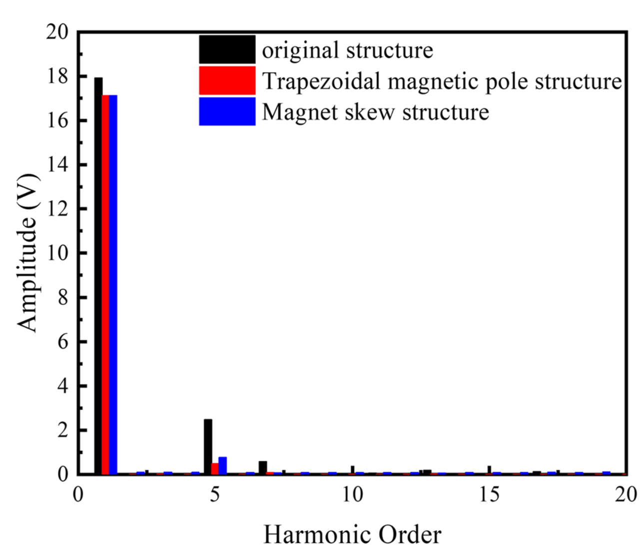

Figure 9: FFT Analysis of the back EMF.

the trapezoidal magnetic pole structure is reduced by 80.4%, and the magnet skew structure is reduced by 69.2%. Among them, the amplitude of the fundamental wave is also reduced to a certain extent, the trapezoidal magnetic pole structure is reduced by about 4.4%, and the magnet skew structure is reduced by about 4.5%. Extract the analysis results, and bring the harmonics of each order into formula (8) to calculate the total harmonic distortion (THD).

$$\mathrm{THD} = \sqrt{\sum_{n=2}^{H}\left(\frac{G_n}{G_1}\right)^2}, \tag{8}$$

where n is the harmonic order, H is the highest harmonic order, G_n is the nth harmonic amplitude, and G_1 is the fundamental wave amplitude. The THD of the original structure motor can be calculated as $(\mathrm{THD})_{\mathrm{original}} = 14.2\%$, the trapezoidal magnetic pole structure motor is $(\mathrm{THD})_{\mathrm{trapezoidal}} = 2.8\%$, and the magnet skew structure motor is $(\mathrm{THD})_{\mathrm{skew}} = 5.3\%$. The THD has been significantly improved after optimization.

3.4 Axial electromagnetic force

Compared with the magnet skew structure motor, the trapezoidal magnetic pole structure motor does not generate axial electromagnetic force due to its axial symmetry. Both use a magnet skew angle of 30°. At the maximum load torque operating point, the axial electromagnetic force comparison of the two motors is shown in Figure 10.

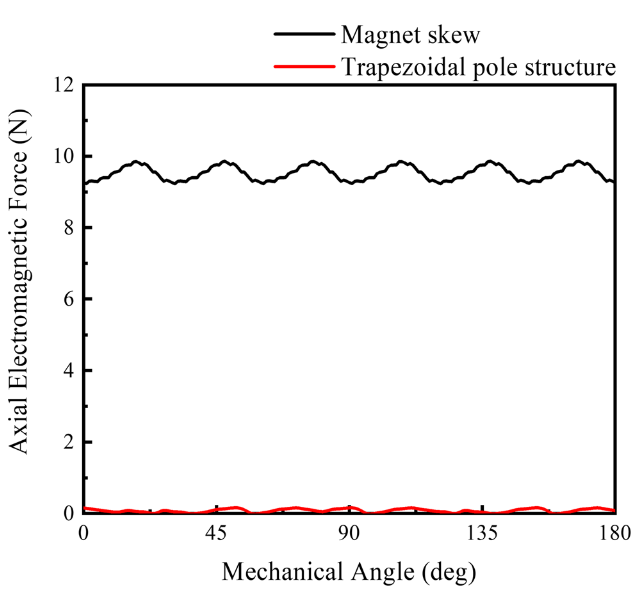

Figure 10: Simulation results of the axial electromagnetic force of the motor.

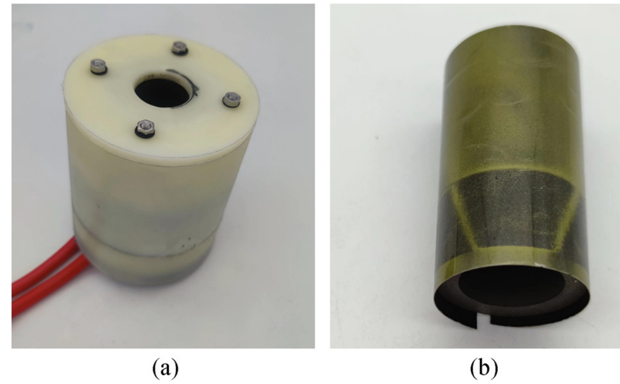

Figure 11: (a) Trapezoidal magnetic pole structure magnetization fixture; (b) trapezoidal magnetic pole structure magnet.

It can be seen that the axial electromagnetic force of the motor using the trapezoidal magnetic pole structure is almost zero. This structure can effectively reduce the cogging torque without generating axial electromagnetic force, effectively prolonging the life of the bearing and reducing small vibration noise, and improve motor control accuracy.

4 Prototype test

In order to further verify the validity of the simulation results, a prototype rotor with trapezoidal magnetic pole structure was made for testing. According to the simulation results above, a trapezoidal magnetic pole structure magnetization fixture with a magnetic pole skew angle $\theta_{\mathrm{sk}} = 30°$ is made, and the magnet ring is magnetized. Figure 11 shows the trapezoidal magnetic pole structure magnetization fixture.

The trapezoidal magnetic pole structure magnet ring is installed and tested, as shown in Figure 12. The one with the white fan in the figure is the trapezoidal

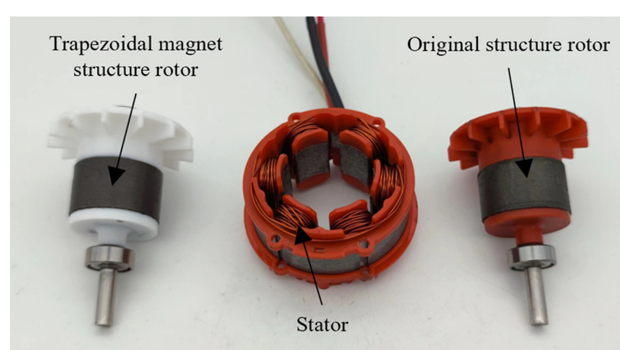

Figure 12: Trapezoidal magnetic pole structure and original structure motor.

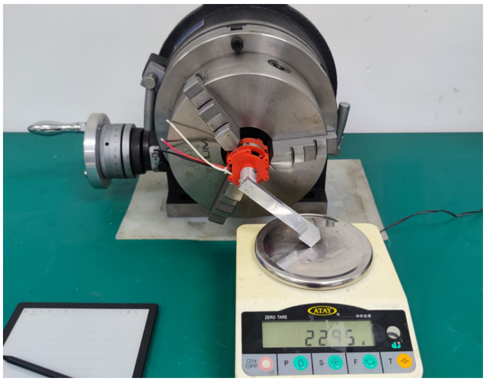

Figure 13: Cogging torque test device.

magnetic pole structure rotor, the red fan is the original structure rotor, and the two rotors use the same stator.

4.1 Cogging torque test

The cogging torque test device is shown in Figure 13.

The test results are shown in Figure 14. Using the trapezoidal magnetic pole structure, the cogging torque is significantly reduced, and the peak-to-peak value is reduced from 77.64 to 9.02 mN m, and the reduction is 88.4%, which is close to the simulation result of 91.3%.

4.2 Back EMF test

Back EMF test device is shown in Figure 15.

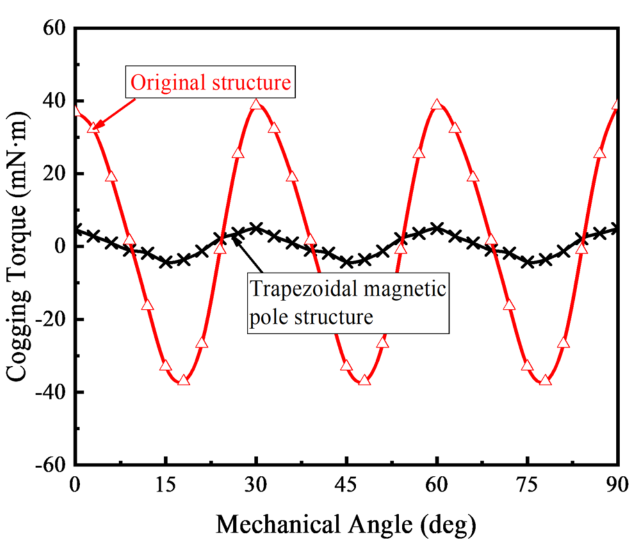

Figure 14: Measured value of cogging torque.

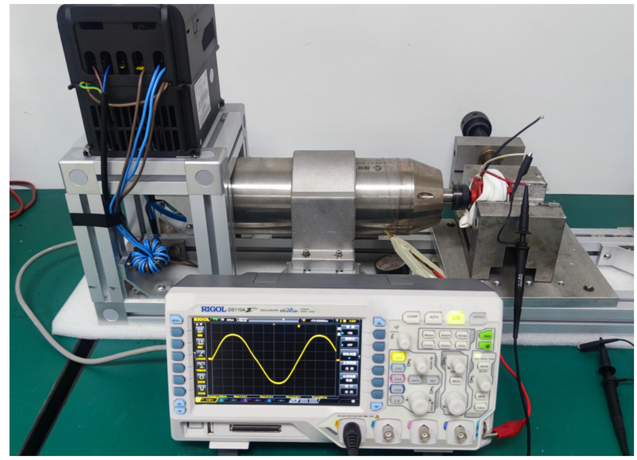

Figure 15: Back EMF test device.

The test results are shown in Figure 16. (a) is the Back EMF of the original structure motor at a speed of 18,000 rpm, and (b) is the Back EMF of the trapezoidal magnetic pole structure motor at a speed of 18,000 rpm.

It can be seen from Figure 16 that the Back EMF waveform of the trapezoidal magnetic pole structure motor is closer to sinusoidal. The Back EMF amplitude

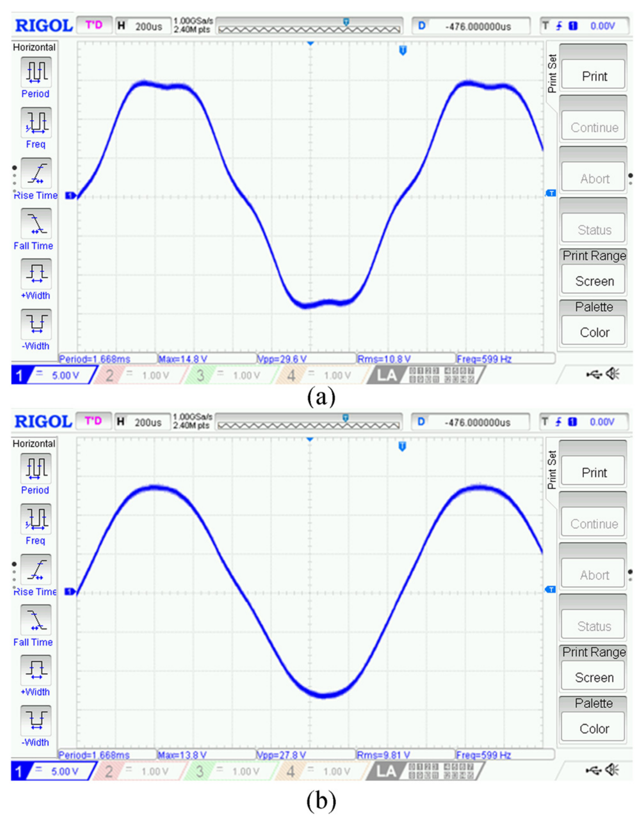

Figure 16: (a) Back EMF of the original structure motor at a speed of 18,000 rpm. (b) Back EMF of the trapezoidal magnetic pole structure motor at a speed of 18,000 rpm.

of the trapezoidal magnetic pole structure is reduced by 6.8%. The simulation result is a decrease of 4.4%, which is close to the simulation results.

5 Conclusions

This article studies the influence of trapezoidal pole distribution on cogging torque of permanent magnet motors. The mechanism of the trapezoidal pole structure weakening the cogging torque of the permanent magnet motor is explained by analytical method, and the calculation formula of the oblique pole angle is derived. In order to further verify the validity of the formula, the trapezoidal magnetic pole structure is tested by combining simulation with experiment. The results show that the trapezoidal pole structure can effectively reduce the cogging torque of permanent magnet motors by more than 90%. Compared with the traditional oblique pole method, the trapezoidal pole structure does not generate additional axial electromagnetic force.

This method can be used to optimize the cogging torque of the permanent magnet motor. Especially in a magnet ring, the trapezoidal magnetic pole structure can be realized only by changing the design of the magnetizing fixture, which will not increase the cost of the manufacturing process of the magnet.

Funding information: This work was supported by the National Key Research and Development Program of China (2021YFB3500201/2021YFB3500202/2021YFB3500205/2022YFB3505503), the Beijing NOVA Program (Z211100002121092), the Natural Science Foundation of Hebei Province (E2021103006), and the Hebei Province International Science and Technology Cooperation Base Construction Project of China (20591002D).

Author contributions: Conceptualization: Zilong Wang, Yang Luo, and Dunbo Yu; funding acquisition: Zilong Wang, Yang Luo, Wenlong Yan, Dunbo Yu, and Li Wang; investigation: Yuanfei Yang; methodology: Ze Zhang and Juntao Yu; software, Ze Zhang; validation: Ze Zhang and Tengfei Hu; writing – original draft: Ze Zhang; writing – review and editing: Ze Zhang and Juntao Yu. All authors have accepted responsibility for the entire content of this manuscript and approved its submission.

Conflict of interest: The authors state no conflict of interest.

References

[1] Fei W, Luk PCK. A new technique of cogging torque suppression in direct-drive permanent-magnet brushless machines. IEEE Trans Ind Appl. 2010;46(4):1332–40.
[2] Dorrell DG, Hsieh MF, Popescu M, Evans L, Staton DA, Grout V. A review of the design issues and techniques for radial-flux brushless surface and internal rare-earth permanent-magnet motors. IEEE Trans Ind Electron. 2011;58(9):3741–57.
[3] Hwang SM, Eom JB, Jung YH, Lee DW, Kang BS. Various design techniques to reduce cogging torque by controlling energy variation in permanent magnet motors. IEEE Trans Magn. 2001;37(4):2806–9.
[4] Jagiela M, Mendrela EA, Gottipati P. Investigation on a choice of stator slot skew angle in brushless PM machines. Electr Eng. 2013;95(3):209–19.
[5] Lukaniszyn M, Jagiela M, Wrobel R. Optimization of permanent magnet shape for minimum cogging torque using a genetic algorithm. IEEE Trans Magn. 2004;40(2):1228–31.
[6] Zhu L, Jiang SZ, Zhu ZQ, Chan CC. Analytical methods for minimizing cogging torque in permanent-magnet machines. IEEE Trans Magn. 2009;45(4):2023–31.
[7] Fei W, Zhu ZQ. Comparison of cogging torque reduction in permanent magnet brushless machines by conventional and herringbone skewing techniques. IEEE Trans Energy Convers. 2013;28(3):664–74.
[8] Wrobel R, Lukaniszyn M, Jagiela M, Latawiec K. A new approach to reduction of the cogging torque in a brushless motor by skewing optimization of permanent magnets. Electr Eng. 2003;85(2):59–69.
[9] Wardach M. Hybrid excited claw pole generator with skewed and non-skewed permanent magnets. Open Phys. 2017;15(1):902–6.
[10] Wang D, Wang X, Yang Y, Zhang R. Optimization of magnetic pole shifting to reduce cogging torque in solid-rotor permanent-magnet synchronous motors. IEEE Trans Magn. 2010;46(5):1228–34.
[11] Goryca Z, Różowicz S, Różowicz A, Pakosz A, Leśko M, Wachta H. Impact of selected methods of cogging torque reduction in multipolar permanent-magnet machines. Energies. 2020;13(22):6108.
[12] Zamani Faradonbeh V, Taghipour Boroujeni S, Takorabet N. Optimum arrangement of PMs in surface-mounted PM machines: cogging torque and flux density harmonics. Electr Eng. 2020;102(3):1117–27.
[13] Goryca Z, Paduszyński K, Pakosz A. Model of the multipolar engine with decreased cogging torque by asymmetrical distribution of the magnets. Open Phys. 2018;16(1):42–5.
[14] Liu T, Huang S, Gao J, Lu K. Cogging torque reduction by slot-opening shift for permanent magnet machines. IEEE Trans Magn. 2013;49(7):4028–31.
[15] Zhu ZQ, Chen JT, Wu LJ, Howe D. Influence of stator asymmetry on cogging torque of permanent magnet brushless machines. IEEE Trans Magn. 2008;44(11):3851–4.
[16] Xintong J, Jingwei X, Yong L, Yongping L. Theoretical and simulation analysis of influences of stator tooth width on cogging torque of BLDC motors. IEEE Trans Magn. 2009;45(10):4601–4.

[17] Joe LE, Nur T. Study the effect of dummy slot in stator and rotor on the cogging torque reduction in permanent magnet machine. IOP Conf Ser Mater Sci Eng. 2020;807(1):012025.
[18] Li R, Shi C, Qu R, Li D, Ren X, Fedida V, et al. A novel modular stator fractional pole-pair permanent-magnet vernier machine with low torque ripple for servo applications. IEEE Trans Magn. 2020;57(2):1–6.
[19] Chen C, Li D, Qu R, Shah MR, Fang H, Fan X, et al. Cogging torque minimization of SMC motor with axially tapered stator tooth tip. 2017 20th International Conference on Electrical Machines and Systems (ICEMS); 2017 Aug 11–14. Sydney, NSW, Australia, Piscataway: IEEE; 2017. p. 1–4.
[20] Wang D, Wang X, Jung SY. Cogging torque minimization and torque ripple suppression in surface-mounted permanent magnet synchronous machines using different magnet widths. IEEE Trans Magn. 2013;49(5):2295–8.
[21] Zhu ZQ, Howe D. Influence of design parameters on cogging torque in permanent magnet machines. IEEE Trans Energy Convers. 2000;15(4):407–12.
[22] Zhang Z, Wang ZL, Yu JT, Yu DB, Luo Y, Yan WL, et al. Comparison of two sinusoidal magnetization modes of bonded magnetic rings. Machines. 2022;10(10):911.
[23] Gao J, Wang G, Liu X, Zhang W, Huang S, Li H. Cogging torque reduction by elementary-cogging-unit shift for permanent magnet machines. IEEE Trans Magn. 2017;53(11):1–5.
[24] Zhu ZQ, Howe D. Analytical prediction of the cogging torque in radial-field permanent magnet brushless motors. IEEE Trans Magn. 1992;28(2):1371–4.
[25] Zhou Y, Li H, Meng G, Zhou S, Cao Q. Analytical calculation of magnetic field and cogging torque in surface-mounted permanent-magnet machines accounting for any eccentric rotor shape. IEEE Trans Ind Electron. 2014;62(6):3438–47.
[26] Ackermann B, Sottek R. Analytical modeling of the cogging torque in permanent magnet motors. Electr Eng. 1995;78(2):117–25.
[27] Gotovac G, Detela A, Lampič G, Valentinčič J. Analytical and FEM approach to reduce the cogging torque in in-wheel motors. Electr Eng. 2015;97(4):269–75.
[28] Shah SQA, Lipo TA, Kwon BI. Modeling of novel permanent magnet pole shape SPM motor for reducing torque pulsation. IEEE Trans Magn. 2012;48(11):4626–9.
[29] Zhao W, Lipo TA, Kwon BI. Material-efficient permanent-magnet shape for torque pulsation minimization in SPM motors for automotive applications. IEEE Trans Ind Electron. 2014;61(10):5779–87.
[30] Kim HJ, Koh CS, Shin PS. A new anisotropic bonded NdFeB permanent magnet and its application to a small DC motor. IEEE Trans Magn. 2010;46(6):2314–7.
[31] Yanai T, Horita S, Nakano M, Tsutsumi S, Fukunaga H. Reduction in flux loss of an Nd-Fe-B bonded ring magnet for an SPM motor. IEEE Trans Magn. 2014;50(11):1–4.
[32] Yang YB, Wang XH, Zhu CQ. Effect of permanent magnet segmentation on the cogging torque of surface mounted permanent magnet motors. Trans China Electrotech Soc. 2012;27(3):73–8.
[33] Bianchi N, Bolognani S. Design techniques for reducing the cogging torque in surface-mounted PM motors. IEEE Trans Ind Appl 2002;38(5):1259–65.